



Published in final edited form as:

*Kidney Int.* 2019 September ; 96(3): 597–611. doi:10.1016/j.kint.2019.03.014.

## Dual lineage tracing shows that glomerular parietal epithelial cells can transdifferentiate toward the adult podocyte fate

Natalya V. Kaverina<sup>1,6</sup>, Diana G. Eng<sup>1,6</sup>, Benjamin S. Freedman<sup>1</sup>, J.Nathan Kutz<sup>2</sup>, Tyler J. Chozinski<sup>3</sup>, Joshua C. Vaughan<sup>3,4</sup>, Jeffrey H. Miner<sup>5</sup>, Jeffrey W. Pippin<sup>1</sup>, Stuart J. Shankland<sup>1</sup>

<sup>1</sup>Division of Nephrology, University of Washington, Seattle, Washington, USA

<sup>2</sup>Department of Applied Mathematics, University of Washington, Seattle, Washington, USA

<sup>3</sup>Department of Chemistry, University of Washington, Seattle, Washington, USA

<sup>4</sup>Department of Physiology and Biophysics, University of Washington, Seattle, Washington, USA

<sup>5</sup>Division of Nephrology, Washington University School of Medicine, St Louis, Missouri, USA

### Abstract

Podocytes are differentiated post-mitotic cells that cannot replace themselves after injury. Glomerular parietal epithelial cells are proposed to be podocyte progenitors. To test whether a subset of parietal epithelial cells transdifferentiate to a podocyte fate, dual reporter *PEC-rtTA* | *LC1* | *tdTomato* | *Nphs1-FLPo* | *FRT-EGFP* mice, named PEC-PODO, were generated. Doxycycline administration permanently labeled parietal epithelial cells with tdTomato reporter (red), and upon doxycycline removal, the parietal epithelial cells (PECs) cannot label further. Despite the presence or absence of doxycycline, podocytes cannot label with tdTomato, but are constitutively labeled with an enhanced green fluorescent protein (EGFP) reporter (green). Only activation of the *Nphs1-FLPo* transgene by labeled parietal epithelial cells can generate a yellow color. At day 28 of experimental focal segmental glomerulosclerosis, podocyte density was 20% lower in 20% of glomeruli. At day 56 of experimental focal segmental glomerulosclerosis, podocyte density was 18% lower in 17% of glomeruli. TdTomato<sup>+</sup> parietal epithelial cells were restricted to Bowman's capsule in healthy mice. However, by days 28 and 56 of experimental disease, two-thirds of tdTomato<sup>+</sup> parietal epithelial cells within glomerular tufts were yellow in color. These cells co-expressed the podocyte markers podocin, nephrin, p57 and VEGF164, but not markers of endothelial (ERG) or mesangial (Perlecan) cells. Expansion microscopy showed primary, secondary and minor processes in tdTomato<sup>+</sup>EGFP<sup>+</sup> cells in glomerular tufts. Thus, our studies provide strong evidence that parietal epithelial cells serve as a source of new podocytes in adult mice.

**Correspondence:** Stuart J. Shankland, Division of Nephrology, Department of Medicine, University of Washington School of Medicine, Box 358058, 750 Republican Street, Seattle, Washington 98109, USA stuartjs@uw.edu.

<sup>6</sup>NVK and DGE contributed equally to this work.

#### DISCLOSURE

All the authors declared no competing interests.

Supplementary material is linked to the online version of the paper at [www.kidney-international.org](http://www.kidney-international.org).

## Keywords

Bowman's capsule; *Cre-Lox*; enhanced green fluorescent protein; *FLP-FRT*; focal segmental glomerulosclerosis; reporter; tdTomato; transdifferentiation

The biological role of glomerular PECs in health and disease is becoming better understood<sup>1</sup> as a result of the ability to lineage trace PECs in mice,<sup>2</sup> the identification of cell markers that distinguish PECs, and the isolation and characterization of cultured PECs.<sup>3,4</sup> From these advances, new knowledge has emerged of the various roles PECs play in the pathogenesis of glomerular scarring<sup>5-7</sup> and the potential role of PECs as podocyte progenitors for adolescent mice<sup>2,8,9</sup> and as progenitors for new adult podocytes following loss in disease.<sup>10-13</sup>

Lineage tracing using inducible reporters is the gold standard for mapping the migration of a permanently prelabeled cell population and determining its fate. The most common system is *Cre-Lox* based, which utilizes a bacteriophage P1 enzyme to mediate the recombination of loxP recognition sequences and turns on reporter expression in a cell population of interest.<sup>14,15</sup> The *Cre-Lox* system can be combined with a Tet-On system, which utilizes a reverse tetracycline-controlled transactivator (rtTA) that recognizes the tetO sequences of the tetracycline response element in the presence of the ligand doxycycline. Another alternative includes the flippase–recognition target (*FLP-FRT*)–mediated recombination system, based on the FLP recombinase from yeast; however, it is un-common for transgenic animals to utilize this system.

To date there are few studies in humans of potential podocyte gain because of the lack of genetic methodologies, although some evidence has been published.<sup>16</sup> In rodents, transgenic methodologies proving that one cell type trans-differentiates to another are limited. Studies outside of the kidney utilize intersectional or subtractive fate mapping, but neither allow for continual tracing of 2 distinct cell populations.<sup>17,18</sup> An unexplored option is to simultaneously utilize both *Cre-Lox* and *FLP-FRT* recombinase systems, which can act independently and thus be used within the same animal and in fact the same cell.

To provide proof that PECs transdifferentiate to a podocyte fate in adult mice after podocyte depletion, we generated dual PEC-podocyte reporter mice. We demonstrate that during the migration of labeled PECs to the glomerular tuft after podocyte loss, a subset activated the *Nphs1-FLPo* promoter, which induced the constitutive labeling with a second reporter, resulting in co-expression of 2 independent reporters.

## RESULTS

### Dual labeling of PECs and podocytes in healthy PEC-PODO mice

The schema used to generate dual *PEC-rtTA|LC1|tdTomato|Nphs1-FLPo|FRT-EGFP* (PEC-PODO) reporter mice is shown in Figure 1a–d. Confocal microscopy confirmed that in healthy adult mice that received doxycycline, 58% ± 12% of cells lining Bowman's capsule expressed tdTomato fluorescent protein (red) in a classic PEC distribution along Bowman's capsule (Figure 1e). A subset of cells in the same glomerular tuft expressed EGFP in a classic podocyte distribution (Figure 1e), and 95% of EGFP<sup>+</sup> cells co-expressed the

podocyte marker p57. Both tdTomato and EGFP were visualized without detecting antibodies.

Staining for the podocyte marker podocin (blue) overlapped with EGFP but not with tdTomato (Figure 1f). Staining for the PEC marker src-suppressed C-kinase substrate (SSeCKS)<sup>19</sup> overlapped with tdTomato but not with EGFP (Figure 1g). When standard chow lacking doxycycline was provided, PEC-PODO mice expressed EGFP but not tdTomato (Supplementary Figure S1A). When mice lacking FLPo were given doxycycline, tdTomato was expressed, but EGFP was not expressed (Supplementary Figure S1B). When mice lacking rtTA were given doxycycline, EGFP was expressed, but tdTomato was not expressed (Supplementary Figure S1C). Following withdrawal of doxycycline after the induction period, the expression of both reporters could only occur when an existing labeled PEC (inducible reporter) constitutively activated the *Nphs1-FLPo* promoter, minimizing the chance of an existing podocyte becoming red and being mistaken for a migrated PEC. To control for the off chance that the disease-inducing cytopathic antibody might induce aberrant tdTomato expression, the antibody was administered to mice that were not given doxycycline. As expected, after podocyte depletion, there was no tdTomato expression and no yellow cells.

These results show that administration of doxycycline to healthy adult PEC-PODO mice inducibly labeled PECs with tdTomato. Podocytes constitutively labeled with EGFP, with no overlap of the 2 reporters (yellow), and thus successful labeling of 2 distinct cell types occurred within the same kidney glomerulus.

### Characteristics of experimental disease model in dual PEC-PODO reporter mice

Experimental focal segmental glomerulosclerosis (FSGS), typified by abrupt podocyte depletion and proteinuria, was induced by administering a cytopathic antipodocyte antibody (see Supplementary Methods) in dual PEC-PODO mice that were given doxycycline as adults, as previously reported.<sup>20–23</sup> Importantly, each mouse underwent a baseline kidney biopsy prior to disease induction to record PEC and podocyte labeling and quantitate podocyte density and PEC size. Temporal changes in each individual mouse were followed between baseline and death at day 28 or 56, when an average of 163 glomeruli per mouse were analyzed.

Injury was defined as reduced podocyte number and increased matrix accumulation, as previously reported.<sup>7,24</sup> As expected, at baseline, 100% of glomeruli were uninjured (Supplementary Figure S2A). At day 28 of FSGS, 20% ± 5% of glomeruli were injured (80% ± 8% were uninjured). At day 56 of FSGS, 17% ± 6% of glomeruli were injured (83% ± 5% were uninjured; Supplementary Figure S2A).

Within injured glomeruli at day 28, podocyte density was 20% ± 5% lower in injured glomeruli ( $216 \pm 5$  vs.  $276 \pm 11 \times 10^6$  podocytes/ $\mu\text{m}^3$  glomerular tuft volume,  $P < 0.05$  vs. uninjured glomeruli; Supplementary Figure S2B), similar to previous reports.<sup>24,25</sup> At day 56, podocyte density in injured glomeruli remained similar to that on day 28 ( $235 \pm 16$  vs.  $286 \pm 15 \times 10^6$  podocytes/ $\mu\text{m}^3$  glomerular tuft volume,  $P < 0.05$  vs. uninjured glomeruli,  $P >$

0.05 vs. day 28). Albumin-to-creatinine ratio increased and then gradually decreased as repair occurred (Supplementary Figure S2C).

Taken together, this proteinuric model was typified by podocyte depletion in focally injured glomeruli.

### **A subset of PECs give rise to podocytes after podocyte depletion**

Confocal microscopy was used to visualize tdTomato (labeled PECs) and EGFP (labeled podocytes), without the need for antibodies. Sections were counterstained with collagen IV (blue) to delineate kidney architecture. Z-stacks were taken through 20- $\mu$ m-thick sections to visualize more of each individual glomerulus than can be observed using a “conventional” single thin section. In healthy adult PEC-PODO mice at baseline, tdTomato<sup>+</sup> PECs were restricted to Bowman’s capsule, and EGFP<sup>+</sup> podocytes were restricted to the glomerular tuft (Figure 2a). At FSGS day 28, EGFP decreased (Figure 2b, Figure 3a–f, and Supplementary Figure S3). Within these glomeruli, tdTomato<sup>+</sup> PECs were visualized on the tuft and yellow cells were detected along Bowman’s capsule and in the glomerular tuft (Figure 2b, Figure 3a–f, and Supplementary Figure S3). The smaller image panels show that yellow cells were due to the overlap of the 2 reporters. At FSGS day 56, EGFP also decreased in injured glomeruli, and tdTomato<sup>+</sup> PECs were detected on the tuft. Similar to day 28, yellow cells were detected along Bowman’s capsule and in the tuft (Figure 2c, Figure 4a–f, and Supplementary Figure S4).

We defined transdifferentiation of tdTomato<sup>+</sup> PECs to a podocyte fate when a red cell on the glomerular tuft also expressed EGFP, becoming yellow. TdTomato<sup>+</sup> only cells were consistent, with PECs not having transdifferentiated to a podocyte fate (undifferentiated PEC). Quantitation was performed for both. Neither red nor yellow cells were detected in uninjured glomeruli with normal podocyte density at days 28 and 56.

At day 28 of FSGS, tdTomato<sup>+</sup> PECs were detected on the tuft in  $59\% \pm 8\%$  of the  $20\% \pm 5\%$  of injured glomeruli. In 36% of these glomeruli, PECs remained undifferentiated (red), and in 23% of these glomeruli, PECs transdifferentiated (turned yellow). The average number of undifferentiated tdTomato<sup>+</sup> PECs in injured glomeruli was  $2.6 \pm 0.3$ /glomerular cross section. The average number of PECs that activated the *Nphs1-FLPo* promoter and turned yellow was  $2.1 \pm 1$ /cross section of injured glomeruli.

At day 56 of FSGS, tdTomato<sup>+</sup> PECs were detected on the tufts in 50% of the  $17\% \pm 6\%$  of injured glomeruli (Figure 5a–c). In 32% of these glomeruli, PECs remained undifferentiated (red), and in 18% PECs transdifferentiated (turned yellow). The average number of undifferentiated tdTomato<sup>+</sup> PECs in injured glomeruli was  $2.1 \pm 0.4$ . The average number of PECs that activated the *Nphs1-FLPo* promoter and turned yellow was  $1.5 \pm 0.3$ .

### **Transdifferentiated PECs co-express several podocyte proteins and VEGF164**

To test whether yellow PECs on the glomerular tuft showed additional evidence of transdifferentiation, co-staining was performed with antibodies to the podocyte markers podocin, nephrin, and p57. Confocal microscopy showed that the vast majority of EGFP<sup>+</sup> tdTomato<sup>+</sup> PECs (yellow) that migrated to the glomerular tuft at days 28 and 56 co-

expressed podocin (Figure 5a–c), nephrin (Figure 6a–c), or p57 (Figure 7a–c). EGFP<sup>+</sup> tdTomato<sup>+</sup> PECs did not co-stain for the endothelial cell marker erythroblast transformation specific-related gene (ERG; Supplementary Figure S5) or the mesangial cell marker perlecan (Supplementary Figure S6).

VEGF164 expression is a synthetic function of podocytes,<sup>26</sup> and thus de novo expression was assessed. TdTomato<sup>+</sup> PECs along Bowman's capsule did not stain for VEGF164 (Figure 8a). However, a subset of EGFP<sup>+</sup> tdTomato<sup>+</sup> PECs on the glomerular tuft co-express VEGF164 (Figure 8b), providing further evidence that a subset of PECs transdifferentiated to a podocyte fate at both days 28 and 56 after podocyte depletion.

### **PECs migrating to the glomerular tuft acquire primary, secondary, and minor processes**

Expansion microscopy, which uses a swellable polymer hydrogel to physically expand fixed specimens for imaging at high spatial resolution, was utilized to determine if a subset of EGFP<sup>+</sup> tdTomato<sup>+</sup> PECs acquired ultrastructural features of podocytes.<sup>27</sup> Figure 9a–e shows a representative confocal Z-stack at day 28 of FSGS of a EGFP<sup>+</sup> tdTomato<sup>+</sup> PEC (yellow) in the glomerular tuft, with projections resembling primary, secondary, and minor processes, which were clearly resolved using this technique. Moreover, the yellow processes interdigitate with those of resident green podocytes (Figure 9f and g). These results show that EGFP<sup>+</sup> tdTomato<sup>+</sup> PECs acquire ultrastructural features of podocytes.

### **Labeled PECs decrease along Bowman's capsule after their migration to the glomerular tuft, but PEC size is unchanged**

To determine the impact of migration on tdTomato<sup>+</sup> PEC number and size, tdTomato<sup>+</sup> PEC density and cell size were measured (Supplementary Figure S7). The density of tdTomato<sup>+</sup> PECs along Bowman's capsule in uninjured glomeruli at FSGS day 28 ( $1.3 \pm 0.1$  labeled PECs/100 mm of Bowman's capsule length) was similar to that of healthy glomeruli at baseline ( $1.4 \pm 0.1$  tdTomato<sup>+</sup> PECs/100 mm of Bowman's capsule length,  $P > 0.05$ ; Supplementary Figure S7), where  $58\% \pm 12\%$  of PECs were labeled with tdTomato. At FSGS day 28, in injured glomeruli, tdTomato<sup>+</sup> PECs (labeled only during the temporal window of doxycycline administration) migrated to the tuft, and therefore the density along Bowman's capsule decreased by 41% from baseline ( $0.8 \pm 0.1$  vs.  $1.4 \pm 0.1$  tdTomato<sup>+</sup> PECs/100 mm of Bowman's capsule  $P = 0.05$ ; Supplementary Figure S7D). Similarly, at FSGS day 56, the density of tdTomato<sup>+</sup> PECs along Bowman's capsule in injured glomeruli decreased by 32% from baseline ( $0.9 \pm 0.1$  vs.  $1.4 \pm 0.1$  tdTomato<sup>+</sup> PECs/100  $\mu\text{m}$  of Bowman's capsule  $P > 0.05$ ; Supplementary Figure S7D).

PEC size also was measured, and the size of tdTomato<sup>+</sup> PECs along Bowman's capsule did not increase in disease, suggesting no PEC hypertrophy in this model (Supplementary Figure S7F).

### **Transdifferentiating PECs do not co-express CD44 and do not proliferate**

CD44, considered a marker of the "activated" profibrotic migratory PEC phenotype,<sup>28</sup> shows no co-staining in tdTomato<sup>+</sup> PECs at baseline (Supplementary Figure S8A). Likewise, CD44 co-staining was not detected in trans-differentiated yellow PECs on the tuft at day 28

of FSGS (Supplementary Figure S8B). This result was not false negative because CD44 co-stained red PECs on Bowman's capsule and on the tuft. Therefore, activated CD44<sup>+</sup> PECs do not seem to differentiate into podocytes, at least while they still express CD44.

Ki-67 was used as a proliferation marker. Staining for Ki-67 was not detected on PEC-derived podocytes (yellow), nor in native podocytes (EGFP<sup>+</sup>; Supplementary Figure S9A). Ki-67 was detected in occasional tdTomato<sup>+</sup> PECs along Bowman's capsule in disease and in the tubulointerstitium, used as an internal positive control (Supplementary Figure S9B). These results support the notion that the subset of PECs that transdifferentiate to a podocyte phenotype are not activated and do not proliferate at the time points studied.

### SIR modeling to better understand PEC transdifferentiation to a podocyte fate

Susceptible, infected, and recovery (SIR) models have been used to model the dynamics of diseases since 1927.<sup>29</sup> Despite their simplicity, they are heavily used in epidemiology as a qualitative way to understand the infection and recovery cycle. The SIR model is commonly used for modeling and predicting infectious disease spread in humans, in endemic diseases, with short infectious periods. Few parameters are necessary to calibrate the model. Importantly, empirical models are valuable when limited data are available and when statistical models are difficult to construct. Recently, the SIR model has been used for several diverse and vast applications.<sup>30</sup>

For our purposes, the SIR model terms represent the following dynamics: S(t) represents the number of healthy podocytes (green), I(t) represents the number of damaged podocytes (purple), and R(t) represents the number of tdTomato<sup>+</sup> PECs (red). Note that a percentage of the tdTomato<sup>+</sup> PECs R(t) turn yellow so that R(t) will be part of S(t). The combination of S(t) + R(t) represents the total number of podocytes in the glomerulus. The classical dynamical model takes the form of a set of differential equations:

$$\frac{dS}{dt} = -bSI$$

$$\frac{dI}{dt} = bSI - kI$$

$$\frac{dR}{dt} = kI$$

where d/dt represents the derivative, or rate of change in time, of the coupling dynamics between the SIR compartments. This set of equations is parameterized by 2 simple parameters, b and k. Indeed, one of the great advantages of this model is that it gives a parsimonious representation of the qualitative dynamics without a high-dimensional overfitting in parameter space. Rather, the b and k can be chosen to be consistent with the observed dynamics.

The schematic in Figure 10 shows the dynamics of healthy podocytes as they are lost as a function of time after disease induction, with  $t(0)$  being the initiation, creating growth in the damaged (infected  $I[t]$  dynamics) podocytes. The recovery variable  $R(t)$  models new podocytes (derived from PECs), which migrated into the glomerulus to replace lost podocytes. If approximately 50% of the migrating PECs change from red to yellow, then the total number of podocytes is the sum of the remaining healthy podocytes  $S(t)$  and 65% of the recovered field  $R(t)$ . The combined dynamics and population of healthy new podocytes are marked yellow.

The findings for this experimental FSGS model show that in “responsive glomeruli” (Supplementary Figure S10) the percentage of native (green) podocytes lost as a result of injury (these are the injured podocytes represented by  $I[t]$ ) was approximately 36%, which leaves approximately 64% in a healthy state (Figure 10a–d). The number of PECs that migrate into the injured glomeruli (red) was 1.9 cells, and the number of PECs that transdifferentiated (turned yellow) in the injured glomeruli was 1.2 cells (a 65% transdifferentiation rate). These numbers align closely to the values in the SIR model simulation.

## DISCUSSION

The extent of podocyte depletion underlies the onset and magnitude of proteinuria and glomerular scarring in glomerular diseases.<sup>31,32</sup> Similar to human disease, the experimental FSGS model employed was proteinuric and focal in nature, involving one fifth of all glomeruli, in which the nadir of podocyte density was depleted by 36%, as we have reported.<sup>21,23,33</sup> Podocyte density then increased by 14% from this nadir, resulting in a “final” podocyte density of  $216 \pm 5$  and  $235 \pm 16 \times 10^6$  podocytes/ $\mu\text{m}^3$  glomerular tuft volume on days 28 and 56, respectively. Because adult podocytes cannot self-replicate, podocyte replacement must derive from other cell sources.<sup>34,35</sup> Limited adult podocyte regeneration has been shown in a diphtheria toxin model of acute podocyte ablation.<sup>9</sup> However, the source of new podocytes was not identified in that study. Glomerular PECs, the focus here, have been shown as a source of new podocytes in several studies: in a cohort of *Pax2.rtTA;TetO.Cre;mT/mG* mice that underwent remission following doxorubicin (Adriamycin) nephropathy<sup>10,36</sup> and in adult *PEC-rtTA/LC1/R26* reporter mice using the same mouse model of FSGS typified by abrupt podocyte depletion described here,<sup>13</sup> which was recently enhanced following CXCL12 blockade in *Pax2.rtTA;TetO.Cre;mT/mG* mice with Adriamycin nephropathy.<sup>36</sup> We acknowledge that certain experimental conditions have failed to show podocyte regeneration. No new podocytes were generated after nephron loss induced by uninephrectomy in *hNPHS2.rtTA;tetO.Cre;mT/mG* mice. This finding is not surprising because this model has no podocyte loss.<sup>9</sup> Similarly, after nephron loss and glomerular hypertrophy in *PEC-rtTA/LC1/R26R* or *PEC-rtTA/H2B-eGFP* transgenic mice, no podocyte regeneration from PECs was observed.<sup>8</sup> Again, podocyte loss is not a feature of this model. However, limited podocyte regeneration was observed after nephron loss in another study.<sup>33</sup>

In the kidney, lineage tracing utilizing the Cre-reporter induction system has been effective in studying podocytes, PECs, tubular epithelial cells, cells of renin lineage, pericytes, and

Gli-1<sup>+</sup> perivascular cells.<sup>34,37-44</sup> In PECs, promoters for truncated podocalyxin<sup>9</sup> or PAX2<sup>10,36</sup> have been used for lineage tracing studies. Thereafter, proving or disproving that labeled PECs transdifferentiate to a podocyte fate has relied on co-staining of labeled PECs with podocyte markers, using antibodies.<sup>8,13</sup> In the current study, we used a new genetic approach in which PECs were inducibly labeled with tdTomato using a Tet-On Cre-based recombinase driven by the truncated podocalyxin promoter,<sup>9</sup> and podocytes were constitutively labeled with EGFP using a FLPo-based recombinase driven by the nephrin promoter.<sup>25</sup> Thus new podocytes derived from PECs became yellow in color. PEC labeling was performed in a temporally restricted way, prior to experimental interventions. In healthy mice labeled as adults (age 4 months), tdTomato co-localized with SSeCKS in 58% of PECs and EGFP co-localized with p57 in approximately 95% of podocytes, with no merge of the 2 reporters detected in the glomerular tuft.

Several observations were made after disease induction. In uninjured glomeruli with no change in podocyte density, no scarring was detected at either day 28 or 56, tdTomato fluorescence remained localized to Bowman's capsule, and no yellow cells were observed in the glomerular tuft. In injured glomeruli with lower podocyte density at both days 28 and 56, tdTomato-labeled PECs were detected on the glomerular tuft, as we reported.<sup>13,45</sup> The first major finding was that yellow cells were detected both in the glomerular tuft and along Bowman's capsule at similar amounts at both days 28 and 56; therefore, the approach used proved that a subset of PECs activated the *Nphs1-FLPo* promoter.

A second finding was that a majority of yellow cells on the glomerular tuft had additional characteristics supporting PEC transdifferentiation to podocytes: (i) the co-expression of the podocyte-specific proteins podocin, nephrin, and p57 but not markers of endothelial (ERG) or mesangial cells (Perlecan); (ii) the de novo expression of VEGF164, a synthetic function of podocytes;<sup>26</sup> (iii) the presence of primary, secondary, and minor processes viewed by expansion microscopy, with the interdigitation with native/resident green podocytes; and (iv) downregulation of the PEC marker SSeCKS. Together, these additional data support the genetic evidence for PEC transdifferentiation to podocytes after podocyte depletion.

Some tdTomato<sup>+</sup> PECs along Bowman's capsule activated the *Nphs1-FLPo* promoter prior to migration to the glomerular tuft. Quantitative analysis showed ~30% of glomeruli had one or more yellow PEC along Bowman's capsule at baseline, which increased to 51% ± 11% at day 28 and 44% ± 8% at day 56 of FSGS. This finding fits well with previous reports of "parietal podocytes"<sup>39,46-50</sup> or "transitional PECs"<sup>51-54</sup> along Bowman's capsule. Although the underlying mechanisms were not explored, lineage tracing during nephrogenesis in PAX8cre β-catenin-deficient mice indicated that β-catenin/Wnt signaling was likely involved.<sup>55</sup> It is likely "parietal podocytes" or "transitional PECs" eventually move to the glomerular tuft, as both tdTomato<sup>+</sup> PECs and EGFP<sup>+</sup> tdTomato<sup>+</sup> PECs decrease along Bowman's capsule.

The labeling efficiency of PECs was 58% (not the ideal 100%). We acknowledge this drawback, because we are likely missing a large percentage of migrating and transitioning PECs, as 42% of PECs were not labeled. Taking this factor into account, the number of migrated PECs may actually be 5. Our calculated transition rate was 65%, which would



result in an average of 4 podocytes being replaced by PECs in responsive glomeruli. Given that a healthy glomerular cross section has on average 12 podocytes, of which 5 are lost, a replacement of 4 podocytes on average results in 11 podocytes in recovering glomeruli, which is 91% of their healthy number.

Additional noteworthy results deserve discussion. First, in glomeruli with tdTomato<sup>+</sup> PECs on the tuft, there was a 41% decrease in the density of tdTomato<sup>+</sup> PECs along Bowman's capsule. The finding was consistent with the migration of the limited population of red PECs labeled during the temporal window of doxycycline administration. Recall that any new PECs replacing a migrated tdTomato<sup>+</sup> PEC by proliferation, as we and others have shown,<sup>7,13,56</sup> could not be labeled. Second, EGFP<sup>+</sup> tdTomato<sup>+</sup> PECs on Bowman's capsule or in the glomerular tuft did not co-express CD44 or the proliferation marker Ki-67, indicating that activated PECs do not differentiate into podocytes, at least while still expressing CD44. Third, PECs along Bowman's capsule did not undergo hypertrophy. These data suggest that the subpopulation of PECs that initially replace podocytes do not express the activated proliferative phenotype that is associated with the generation of glomerular scarring,<sup>5,7,13,28</sup> and CD44 is unlikely to be a "stemness" marker for PECs as in other cell types.<sup>57</sup>

One limitation of this technique is that it requires sophisticated crosses to produce a small number of animals, which are informative yet precious. The ideal lineage tracing experiment would be the use of 2 inducible reporter systems. However, to track the active transition of a PEC to a podocyte in a dual inducible system, the podocyte induction agent must be present throughout the entire disease and repair processes. This requirement defeats the purpose behind a dual inducible system, because the presence of the induction reagent throughout the study would create a situation similar to the constitutive system. As a result of podocyte injury in this model, EGFP could leak and be taken up by other cells. In fact, faint EGFP was noted in proximal tubular cells, coinciding with proteinuria. However, if this was indeed responsible for the changes observed, one would expect to see EGFP in all PECs, as well as other glomerular cells (mesangial or endothelial cells). EGFP observed in PECs was only in a portion of cells and the signal was strong, similar to the targeted labeling in podocytes. Furthermore, EGFP was not observed in any other glomerular cells. Therefore, we believe the lineage tracing system we used performed appropriately. However, we recognize the limitation that aberrant direct labeling of PECs as "podocytes" cannot be ruled out in the current studies and its impact on the results are unknown and might even be viewed as controversial. Why certain PECs transdifferentiate while others do not is a key question. Previous studies suggest different subpopulations of PEC progenitors lining Bowman's capsule.<sup>58-61</sup> In future studies, the strategy described might be developed to purify and segregate distinct subpopulations of PECs.

In summary, these studies in adult dual PEC-PODO mice provide direct evidence that after abrupt podocyte depletion, a subset of PECs can activate the *Nphs1-FLPo* promoter and transdifferentiate to a podocyte fate defined as the *de novo* coexpression of 3 podocyte markers, *de novo* expression of VEGF164, and development of primary, secondary, and minor processes. Dual PEC-PODO reporter mice provide a new methodology to lineage trace podocytes and PECs simultaneously, within the same glomerulus, in the context of glomerular disease.

## METHODS

### Animals

Dual reporting *PEC-rtTA/LC1/tdTomato/Nphs1-FLPo/FRT-EGFP* (PEC-PODO) mice were produced by crossing previously reported PEC-reporter mice<sup>6,8,13,62</sup> with the tdTomato Ai14 mouse (JAX #007914).<sup>63</sup> Control mice consisted of quadruple transgenic mice without the rtTA or FLPo. Mice were housed in the animal care facility of the University of Washington under specific pathogen-free conditions. Studies were approved by the University of Washington Institutional Animal Care and Use Committee (2968–04). See Supplementary Methods for details.

### Reporter induction

Mice were randomized into labeled and control (nonlabeled) groups. Permanent labeling of PECs was induced by providing ad libitum 625 mg/kg doxycycline chow (Harlan TD.01306, Harlan Laboratories, Indianapolis, IN) for 3 weeks followed by a washout period of 1 week.

### Experimental FSGS

Experimental FSGS was induced by 2 intraperitoneal injections, 24 hours apart, of a cytopathic sheep anti-glomerular antibody (12 mg/20 g body weight), which induces podocyte loss by inducing apoptosis<sup>64</sup> and detachment.<sup>65</sup> Spot urine was collected at baseline and after days 1, 3, 5, 7, 10, 14, 21, 28, 35, 42, 49, and 56 of FSGS. Urine albumin was determined using an albumin RID assay.<sup>66</sup> Urine creatinine was determined using a colorimetric microplate assay (Cayman Chemical, Ann Arbor, MI).

### Tissue collection

All mice underwent a survival biopsy (see Supplementary Methods). For terminal kidney necropsies, mice were killed as previously described,<sup>22</sup> at days 28 ( $n = 4$ ) and 56 ( $n = 10$ ).

### Visualization of dual (tdTomato/EGFP) reporter

TdTomato and EGFP fluorescent reporters did not require detecting antibodies for visualization. Confocal images were acquired with a Leica TCS SPE II laser scanning confocal microscope (Solms, Germany) with  $\times 40$  (1.3 NA) oil objective. See Supplementary Methods for details.

### Measuring podocyte density, PEC density, and PEC size

Podocyte density was measured by the previously reported correction factor method.<sup>67</sup> PEC size was measured using the karyoplasmic ratio.<sup>68–70</sup> See Supplementary Methods for details.

### Multicolor immunofluorescence staining

Immunostaining was performed on 20- $\mu$ m sections from 4% paraformaldehyde-fixed frozen and paraffin sections as previously described.<sup>22</sup> See Supplementary Methods for details.

## Expansion of a kidney specimen using expansion microscopy

Expansion microscopy was performed by using a previously described protocol.<sup>27</sup> See Supplementary Methods for details.

## Microscopy

Images were detected on a Leica TCS SPE II laser scanning confocal microscope using 400 × magnification. Expansion microscopy was performed on a Leica SP5 inverted confocal point scanning microscope at the UW Biology Imaging Core. See Supplementary Methods for details.

## Statistical analyses

Data are shown as the mean ± SEM. The Student t-test was applied for comparisons between groups. Multiple groups were compared using one-way analysis of variance with the post hoc Tukey honestly significant difference test. *P* values <0.05 represented statistically significant differences.

## Supplementary Material

Refer to Web version on PubMed Central for supplementary material.

## ACKNOWLEDGMENTS

This research was supported by National Institutes of Health (NIH) grants 5 R01 DK 056799–10, 5 R01 DK Q24056799–12, 1 R01 DK097598–01A1, 1 UH2DK107343–02, NIDDK Diabetic Complications Consortium grant DK115255, and NIH R01 MH115767 (JCV) and NSF Graduate Research Fellowship DGE-1256082 (TJC).

## REFERENCES

1. Chang AM, Ohse T, Krofft RD, et al. Albumin-induced apoptosis of glomerular parietal epithelial cells is modulated by extracellular signal-regulated kinase 1/2. *Nephrol Dial Transplant*. 2012;27:1330–1343. [PubMed: 21896500]
2. Appel D, Kershaw DB, Smeets B, et al. Recruitment of podocytes from glomerular parietal epithelial cells. *J Am Soc Nephrol*. 2009;20:333–343. [PubMed: 19092119]
3. Ohse T, Pippin JW, Vaughan MR, et al. Establishment of conditionally immortalized mouse glomerular parietal epithelial cells in culture. *J Am Soc Nephrol*. 2008;19:1879–1890. [PubMed: 18596122]
4. Kabgani N, Grigoleit T, Schulte K, et al. Primary cultures of glomerular parietal epithelial cells or podocytes with proven origin. *PLoS One*. 2012;7:e34907.
5. Eymael J, Sharma S, Loeven MA, et al. CD44 is required for the pathogenesis of experimental crescentic glomerulonephritis and collapsing focal segmental glomerulosclerosis. *Kidney Int*. 2018;93:626–642. [PubMed: 29276101]
6. Smeets B, Kuppe C, Sicking EM, et al. Parietal epithelial cells participate in the formation of sclerotic lesions in focal segmental glomerulosclerosis. *J Am Soc Nephrol*. 2011;22:1262–1274. [PubMed: 21719782]
7. Roeder SS, Barnes TJ, Lee JS, et al. Activated ERK1/2 increases CD44 in glomerular parietal epithelial cells leading to matrix expansion. *Kidney Int*. 2017;91:896–913. [PubMed: 27998643]
8. Berger K, Schulte K, Boor P, et al. The regenerative potential of parietal epithelial cells in adult mice. *J Am Soc Nephrol*. 2014;25:693–705. [PubMed: 24408873]
9. Wanner N, Hartleben B, Herbach N, et al. Unraveling the role of podocyte turnover in glomerular aging and injury. *J Am Soc Nephrol*. 2014;25:707–716. [PubMed: 24408871]

10. Lasagni L, Angelotti ML, Ronconi E, et al. Podocyte regeneration driven by renal progenitors determines glomerular disease remission and can be pharmacologically enhanced. *Stem Cell Rep.* 2015;5:248–263.
11. Peired A, Angelotti ML, Ronconi E, et al. Proteinuria impairs podocyte regeneration by sequestering retinoic acid. *J Am Soc Nephrol.* 2013;24: 1756–1768. [PubMed: 23949798]
12. Lasagni L, Ballerini L, Angelotti ML, et al. Notch activation differentially regulates renal progenitors proliferation and differentiation toward the podocyte lineage in glomerular disorders. *Stem Cells.* 2010;28:1674–1685. [PubMed: 20680961]
13. Eng DG, Sunseri MW, Kaverina NV, et al. Glomerular parietal epithelial cells contribute to adult podocyte regeneration in experimental focal segmental glomerulosclerosis. *Kidney Int.* 2015;88:999–1012. [PubMed: 25993321]
14. Wu F Conditional targeting in the kidney. *Nephron Physiol.* 2007;107: p10–p16. [PubMed: 17657166]
15. Chai OH, Song CH, Park SK, et al. Molecular regulation of kidney development. *Anat Cell Biol.* 2013;46:19–31. [PubMed: 23560233]
16. Puelles VG, Douglas-Denton RN, Cullen-McEwen LA, et al. Podocyte number in children and adults: associations with glomerular size and numbers of other glomerular resident cells. *J Am Soc Nephrol.* 2015;26: 2277–2288. [PubMed: 25568174]
17. Jensen P, Dymecki SM. Essentials of recombinase-based genetic fate mapping in mice. *Methods Mol Biol.* 2014;1092:437–454. [PubMed: 24318835]
18. Yamamoto M, Shook NA, Kanisicak O, et al. A multifunctional reporter mouse line for Cre- and FLP-dependent lineage analysis. *Genesis.* 2009;47:107–114. [PubMed: 19165827]
19. Burnworth B, Pippin J, Karna P, et al. SSeCKS sequesters cyclin D1 in glomerular parietal epithelial cells and influences proliferative injury in the glomerulus. *Lab Invest.* 2012;92:499–510. [PubMed: 22249313]
20. Kaverina NV, Eng DG, Schneider RR, et al. Partial podocyte replenishment in experimental FSGS derives from nonpodocyte sources. *Am J Physiol Renal Physiol.* 2016;310:F1397–F1413. [PubMed: 27076646]
21. Lichtnekert J, Kaverina NV, Eng DG, et al. Renin-angiotensin-aldosterone system inhibition increases podocyte derivation from cells of renin lineage. *J Am Soc Nephrol.* 2016;27:3611–3627. [PubMed: 27080979]
22. Kaverina NV, Kadoya H, Eng DG, et al. Tracking the stochastic fate of cells of the renin lineage after podocyte depletion using multicolor reporters and intravital imaging. *PLoS One.* 2017;12:e0173891.
23. Kaverina NV, Eng DG, Largent AD, et al. WT1 is necessary for the proliferation and migration of cells of renin lineage following kidney podocyte depletion. *Stem Cell Rep.* 2017;9:1152–1166.
24. Schneider RR, Eng DG, Kutz JN, et al. Compound effects of aging and experimental FSGS on glomerular epithelial cells. *Aging (Albany NY).* 2017;9:524–546. [PubMed: 28222042]
25. Eng DG, Kaverina NV, Schneider RRS, et al. Detection of renin lineage cell transdifferentiation to podocytes in the kidney glomerulus with dual lineage tracing. *Kidney Int.* 2018;93:1240–1246. [PubMed: 29580637]
26. Eremina V, Quaggin SE. The role of VEGF-A in glomerular development and function. *Curr Opin Nephrol Hypertens.* 2004;13:9–15. [PubMed: 15090854]
27. Chozinski TJ, Mao C, Halpern AR, et al. Volumetric, nanoscale optical imaging of mouse and human kidney via expansion microscopy. *Sci Rep.* 2018;8:10396. [PubMed: 29991751]
28. Fatima H, Moeller MJ, Smeets B, et al. Parietal epithelial cell activation marker in early recurrence of FSGS in the transplant. *Clin J Am Soc Nephrol.* 2012;7:1852–1858. [PubMed: 22917699]
29. Kermack WO, McKendrick AG. Contributions to the mathematical theory of epidemics—I. 1927. *Bull Math Biol.* 1991;53:33–55. [PubMed: 2059741]
30. Hethcote HW. The mathematics of infectious diseases. *Siam Rev.* 2000;42: 599–653.
31. Wharram BL, Goyal M, Wiggins JE, et al. Podocyte depletion causes glomerulosclerosis: diphtheria toxin-induced podocyte depletion in rats expressing human diphtheria toxin receptor transgene. *J Am Soc Nephrol.* 2005;16:2941–2952. [PubMed: 16107576]

32. Wiggins RC. The spectrum of podocytopathies: a unifying view of glomerular diseases. *Kidney Int.* 2007;71:1205–1214. [PubMed: 17410103]
33. Pippin JW, Kaverina NV, Eng DG, et al. Cells of renin lineage are adult pluripotent progenitors in experimental glomerular disease. *Am J Physiol Renal Physiol.* 2015;309:F341–F358. [PubMed: 26062877]
34. Shankland SJ, Freedman BS, Pippin JW. Can podocytes be regenerated in adults? *Curr Opin Nephrol Hypertens.* 2017;26:154–164. [PubMed: 28306565]
35. Shankland SJ, Pippin JW, Duffield JS. Progenitor cells and podocyte regeneration. *Semin Nephrol.* 2014;34:418–428. [PubMed: 25217270]
36. Romoli S, Angelotti ML, Antonelli G, et al. CXCL12 blockade preferentially regenerates lost podocytes in cortical nephrons by targeting an intrinsic podocyte-progenitor feedback mechanism. *Kidney Int.* 2018;94:1111–1126. [PubMed: 30385042]
37. Asano T, Niimura F, Pastan I, et al. Permanent genetic tagging of podocytes: fate of injured podocytes in a mouse model of glomerular sclerosis. *J Am Soc Nephrol.* 2005;16:2257–2262. [PubMed: 15987751]
38. Dai Y, Chen A, Liu R, et al. Retinoic acid improves nephrotoxic serum-induced glomerulonephritis through activation of podocyte retinoic acid receptor alpha. *Kidney Int.* 2017;92:1444–1457. [PubMed: 28756872]
39. Schulte K, Berger K, Boor P, et al. Origin of parietal podocytes in atubular glomeruli mapped by lineage tracing. *J Am Soc Nephrol.* 2014;25:129–141. [PubMed: 24071005]
40. Hamatani H, Eng DG, Kaverina NV, et al. Lineage tracing aged mouse kidneys shows lower number of cells of renin lineage and reduced responsiveness to RAAS inhibition. *Am J Physiol Renal Physiol.* 2018;315: F97–F109. [PubMed: 29412700]
41. Kramann R, Schneider RK, DiRocco DP, et al. Perivascular Gli1 + progenitors are key contributors to injury-induced organ fibrosis. *Cell Stem Cell.* 2015;16:51–66. [PubMed: 25465115]
42. Humphreys BD, Lin SL, Kobayashi A, et al. Fate tracing reveals the pericyte and not epithelial origin of myofibroblasts in kidney fibrosis. *Am J Pathol.* 2010;176:85–97. [PubMed: 20008127]
43. Jiang MH, Li G, Liu J, et al. Nestin(+) kidney resident mesenchymal stem cells for the treatment of acute kidney ischemia injury. *Biomaterials.* 2015;50:56–66. [PubMed: 25736496]
44. Prodromidi EI, Poulosom R, Jeffery R, et al. Bone marrow-derived cells contribute to podocyte regeneration and amelioration of renal disease in a mouse model of Alport syndrome. *Stem Cells.* 2006;24:2448–2455. [PubMed: 16873763]
45. Ohse T, Vaughan MR, Kopp JB, et al. De novo expression of podocyte proteins in parietal epithelial cells during experimental glomerular disease. *Am J Physiol Renal Physiol.* 2010;298:F702–F711. [PubMed: 20007346]
46. Gibson IW, Downie I, Downie TT, et al. The parietal podocyte: a study of the vascular pole of the human glomerulus. *Kidney Int.* 1992;41: 211–214. [PubMed: 1593857]
47. Bariety J, Mandet C, Hill GS, et al. Parietal podocytes in normal human glomeruli. *J Am Soc Nephrol.* 2006;17:2770–2780. [PubMed: 16943305]
48. Gibson IW, Downie TT, More IA, et al. Tuft-to-capsule adhesions and their precursors: differences between the vascular and tubular poles of the human glomerulus. *J Pathol.* 1998;184:430–435. [PubMed: 9664911]
49. Benigni A, Morigi M, Rizzo P, et al. Inhibiting angiotensin-converting enzyme promotes renal repair by limiting progenitor cell proliferation and restoring the glomerular architecture. *Am J Pathol.* 2011;179: 628–638. [PubMed: 21718676]
50. Macconi D, Sangalli F, Bonomelli M, et al. Podocyte repopulation contributes to regression of glomerular injury induced by ACE inhibition. *Am J Pathol.* 2009;174:797–807. [PubMed: 19164508]
51. Zhang J, Pippin JW, Vaughan MR, et al. Retinoids augment the expression of podocyte proteins by glomerular parietal epithelial cells in experimental glomerular disease. *Nephron Exp Nephrol.* 2012;121: e23–e37. [PubMed: 23107969]
52. Zhang J, Hansen KM, Pippin JW, et al. De novo expression of podocyte proteins in parietal epithelial cells in experimental aging nephropathy. *Am J Physiol Renal Physiol.* 2012;302:F571–F580. [PubMed: 22129965]

53. Naito S, Pippin JW, Shankland SJ. The glomerular parietal epithelial cell's responses are influenced by SM22 alpha levels. *BMC Nephrol.* 2014;15:174. [PubMed: 25376243]
54. Zhang J, Pippin JW, Krofft RD, et al. Podocyte repopulation by renal progenitor cells following glucocorticoids treatment in experimental FSGS. *Am J Physiol Renal Physiol.* 2013;304:F1375–F1389. [PubMed: 23486009]
55. Grouls S, Iglesias DM, Wentzensen N, et al. Lineage specification of parietal epithelial cells requires beta-catenin/Wnt signaling. *J Am Soc Nephrol.* 2012;23:63–72. [PubMed: 22021707]
56. Kuppe C, Grone HJ, Ostendorf T, et al. Common histological patterns in glomerular epithelial cells in secondary focal segmental glomerulosclerosis. *Kidney Int.* 2015;88:990–998. [PubMed: 25853334]
57. Mafi P, Hindocha S, Mafi R, et al. Adult mesenchymal stem cells and cell surface characterization —a systematic review of the literature. *Open Orthop J.* 2011;5:253–260. [PubMed: 21966340]
58. Sagrinati C, Netti GS, Mazzinghi B, et al. Isolation and characterization of multipotent progenitor cells from the Bowman's capsule of adult human kidneys. *J Am Soc Nephrol.* 2006;17:2443–2456. [PubMed: 16885410]
59. Romagnani P Family portrait: renal progenitor of Bowman's capsule and its tubular brothers. *Am J Pathol.* 2011;178:490–493. [PubMed: 21281781]
60. Angelotti ML, Ronconi E, Ballerini L, et al. Characterization of renal progenitors committed toward tubular lineage and their regenerative potential in renal tubular injury. *Stem Cells.* 2012;30:1714–1725. [PubMed: 22628275]
61. Lasagni L, Romagnani P. Basic research: Podocyte progenitors and ectopic podocytes. *Nat Rev Nephrol.* 2013;9:715–716. [PubMed: 24217462]
62. Sicking EM, Fuss A, Uhlig S, et al. Subtotal ablation of parietal epithelial cells induces crescent formation. *J Am Soc Nephrol.* 2012;23:629–640. [PubMed: 22282596]
63. Madisen L, Zwingman TA, Sunkin SM, et al. A robust and high-throughput Cre reporting and characterization system for the whole mouse brain. *Nat Neurosci.* 2010;13:133–140. [PubMed: 20023653]
64. Mundel P, Shankland SJ. Podocyte biology and response to injury. *J Am Soc Nephrol.* 2002;13:3005–3015. [PubMed: 12444221]
65. Shankland SJ. The podocyte's response to injury: role in proteinuria and glomerulosclerosis. *Kidney Int.* 2006;69:2131–2147. [PubMed: 16688120]
66. Marshall CB, Krofft RD, Pippin JW, et al. CDK inhibitor p21 is prosurvival in adriamycin-induced podocyte injury, in vitro and in vivo. *Am J Physiol Renal Physiol.* 2010;298:F1140–F1151. [PubMed: 20130121]
67. Venkatareddy M, Wang S, Yang Y, et al. Estimating podocyte number and density using a single histologic section. *J Am Soc Nephrol.* 2014;25: 1118–1129. [PubMed: 24357669]
68. Huber MD, Gerace L. The size-wise nucleus: nuclear volume control in eukaryotes. *J Cell Biol.* 2007;179:583–584. [PubMed: 17998404]
69. Chan YH, Marshall WF. Scaling properties of cell and organelle size. *Organogenesis.* 2010;6:88–96. [PubMed: 20885855]
70. Mukherjee RN, Chen P, Levy DL. Recent advances in understanding nuclear size and shape. *Nucleus.* 2016;7:167–186. [PubMed: 26963026]

**Translational Statement**

Replacing lost adult podocytes in disease is a therapeutic goal to limit and even reverse proteinuria and glomerular scarring. The results from this experimental study add to the body of work that a subpopulation of PECs serves as podocyte progenitors and provides confidence of ongoing efforts to enhance these events in patients with glomerular diseases.

Author Manuscript

Author Manuscript

Author Manuscript

Author Manuscript

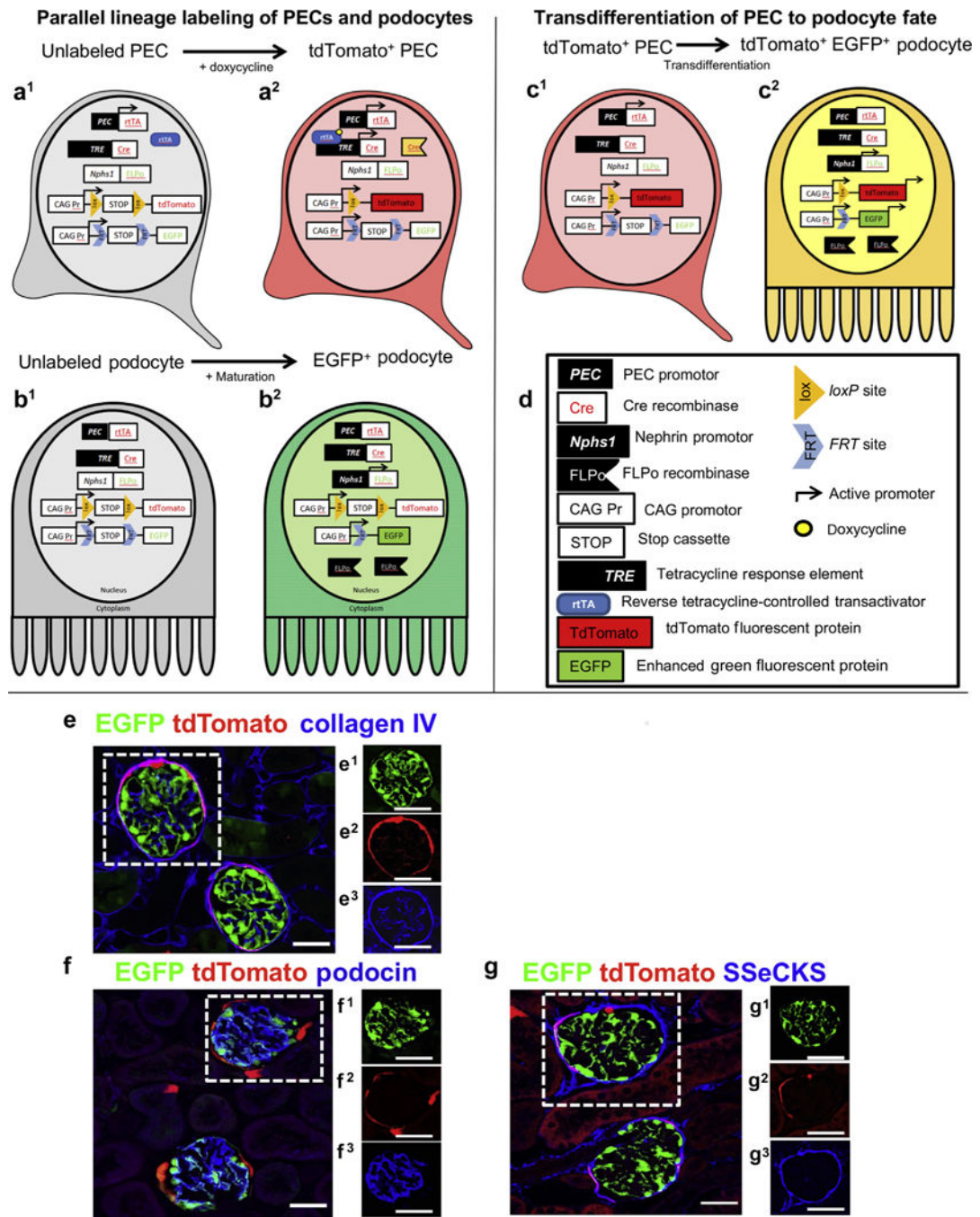


**Figure 1].** Schema and characterization of dual lineage tracing in *PEC-rtTA|LC1|tdTomato|Nphs1-FLPo|FRT-EGFP* (PEC-PODO) transgenic mice.

(a–d) Schema of transgenics. (a1) Unlabeled parietal epithelial cells (PECs) activate the PEC promoter (black box, white type), inducing reverse tetracycline-controlled transactivator (rtTA) expression (white box, red type) in PECs. The rtTA is unable to bind and activate the transcription of the tetracycline response element (tetracycline response element, black box, white type) in the absence of doxycycline, a tetracycline analogue. (a2) When doxycycline (yellow circle) is present, it binds to the ligand-binding domain of the



rtTA, allowing activation of the tetracycline response element, which results in the expression of cre (white box, red type). The expression of cre facilitates the recombination of *loxP* sites (orange triangles, black type), thus removing the intervening STOP cassette (white box, black type), inducing permanent tdTomato (red box, black type) expression. **(b1)** The *Nphs* promoter (white box, black type) in immature podocytes has not yet been activated. **(b2)** During maturation of podocytes, the *Nphs1* promoter is activated (black box, white type), driving FLPase (black flags, white type) expression, which facilitates the recombination of FRT sites (blue chevron, black type) and removal of the intervening STOP cassette (white box, black type), inducing permanent enhanced green fluorescent protein (EGFP; green box, black type) expression. **(c1)** tdTomato<sup>+</sup> PECs have not yet activated the *Nphs1* promoter (white box, black type). **(c2)** Upon transdifferentiation to a podocyte fate, the *Nphs1* promoter is activated (black box, white type), driving FLPase (black flags, white type) expression; FLPase recombines the FRT sites (blue chevron, black type) and STOP cassette (white box, black type), inducing permanent EGFP (green box, black type) expression, resulting in a yellow color. **(e-g)** Confocal microscopy of dual reporter labeling for both PECs and podocytes in the same glomerulus. Reporter labeling following doxycycline administration to healthy adult dual reporting PEC-PODO mice. **(e)** Confocal microscopic image shows PECs expressing tdTomato (red) and podocytes expressing EGFP (green). Antibodies are not required to detect tdTomato or EGFP fluorescence. Collagen IV staining (blue) was used to delineate kidney architecture. Individual green **(e1)**, red **(e2)**, and far-red (blue, **e3**) fluorescent channels of the glomerulus are outlined by the white dashed box in panel **(e)**. **(f)** The podocyte marker podocin (blue) overlaps with EGFP to create a cyan color, but it does not overlap with tdTomato. Individual green **(f1)**, red **(f2)**, and far-red (blue, **f3**) fluorescent channels of the glomerulus are outlined by the white dashed box. **(g)** The PEC marker src-suppressed C-kinase substrate (SSeCKS; blue) overlaps with tdTomato but not EGFP to create a magenta color. Individual green **(g1)**, red **(g2)**, and far-red (blue, **g3**) fluorescent channels of the glomerulus are outlined by the white dashed box. Bars = 25  $\mu$ m.

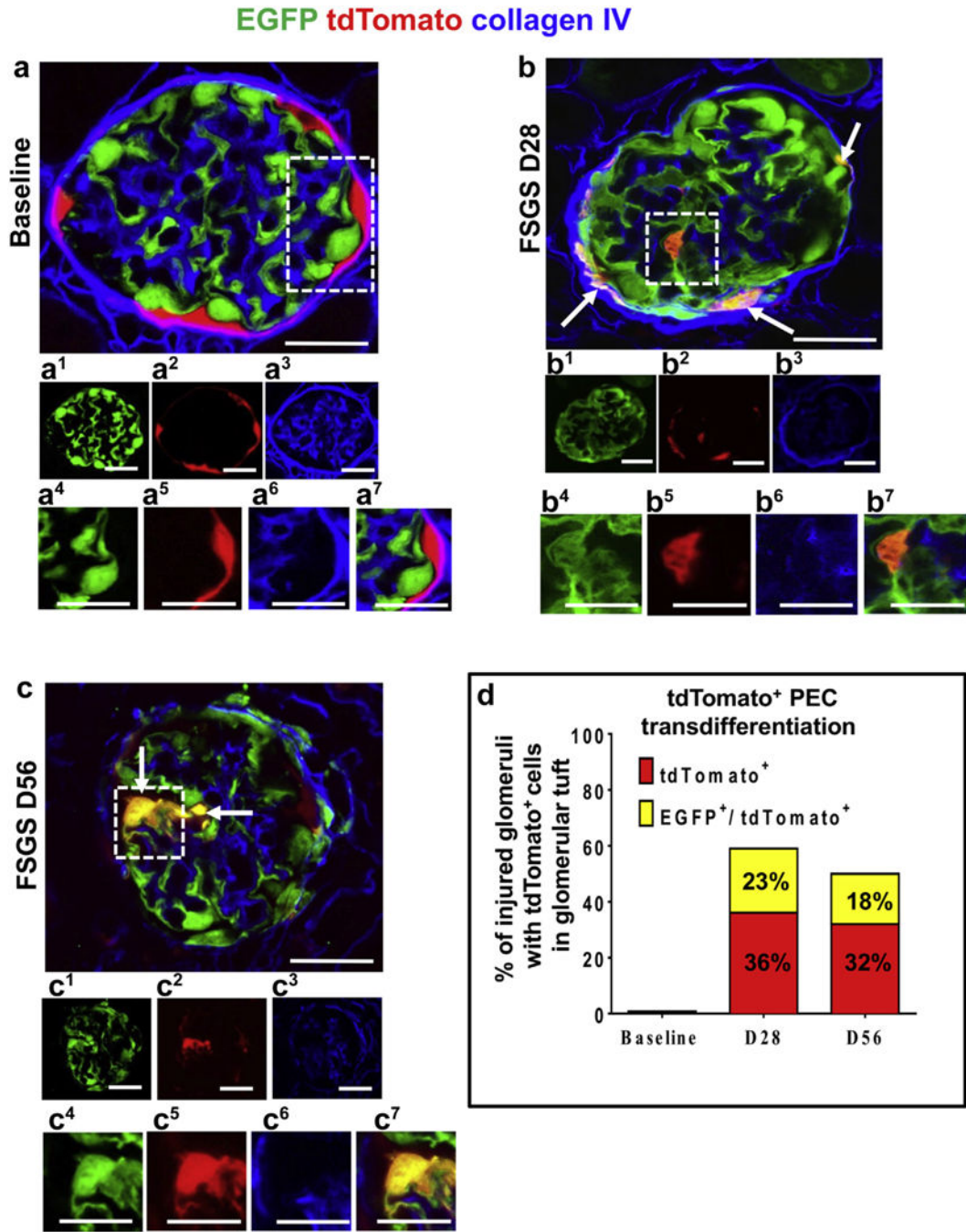


**Figure 2]. Transdifferentiation of parietal epithelial cells (PECs) to a podocyte fate after podocyte depletion.**

(a–c) Confocal microscopic images of enhanced green fluorescent protein (EGFP)<sup>b</sup> podocytes (green), tdTomato<sup>+</sup> PECs (red), podocytes derived from PEC origin (yellow), and collagen IV (blue, used to delineate kidney architecture). In panels labeled with numbers, 1 (green), 2 (red), and 3 (blue) are fluorescent channels of whole glomeruli and 4 (green), 5 (red), 6 (blue), and 7 (merged) are channels of the area outlined by the white dashed boxes. (a) At baseline, tdTomato<sup>+</sup> PECs are limited to Bowman’s capsula and EGFP<sup>+</sup> podocytes to

the glomerular tuft, with no overlap. **(b)** At focal segmental glomerulosclerosis (FSGS) day 28 (D28), a subpopulation of yellow cells are detected along Bowman's capsule (arrows) and on the glomerular tuft (within the dashed box). **(c)** At FSGS day 56 (D56), yellow cells (arrows) are detected on the glomerular tuft (marked with dashed box). There is an overall decrease in EGFP<sup>+</sup> podocytes, and fewer tdTomato<sup>+</sup>PECs are detected along Bowman's capsule. **(d)** Quantitative analysis of the percentage of injured glomeruli with tdTomato<sup>+</sup> PECs in the glomerular tuft. tdTomato<sup>+</sup> PECs (red) and PECs that transdifferentiated to a podocyte fate (yellow) were not detected in the glomerular tuft in baseline glomeruli nor in uninjured glomeruli at FSGS day 28 and day 56. Of the subset of injured glomeruli, 36% had 1 or more undifferentiated tdTomato<sup>+</sup> PECs (red), whereas 23% of the injured glomeruli had transdifferentiated PECs (yellow) at day 28 of FSGS. At day 56, 32% of the injured glomeruli had undifferentiated tdTomato<sup>+</sup> PECs (red) and 18% had transdifferentiated PECs (yellow). Bars = 25  $\mu$ m or 5  $\mu$ m (insets).

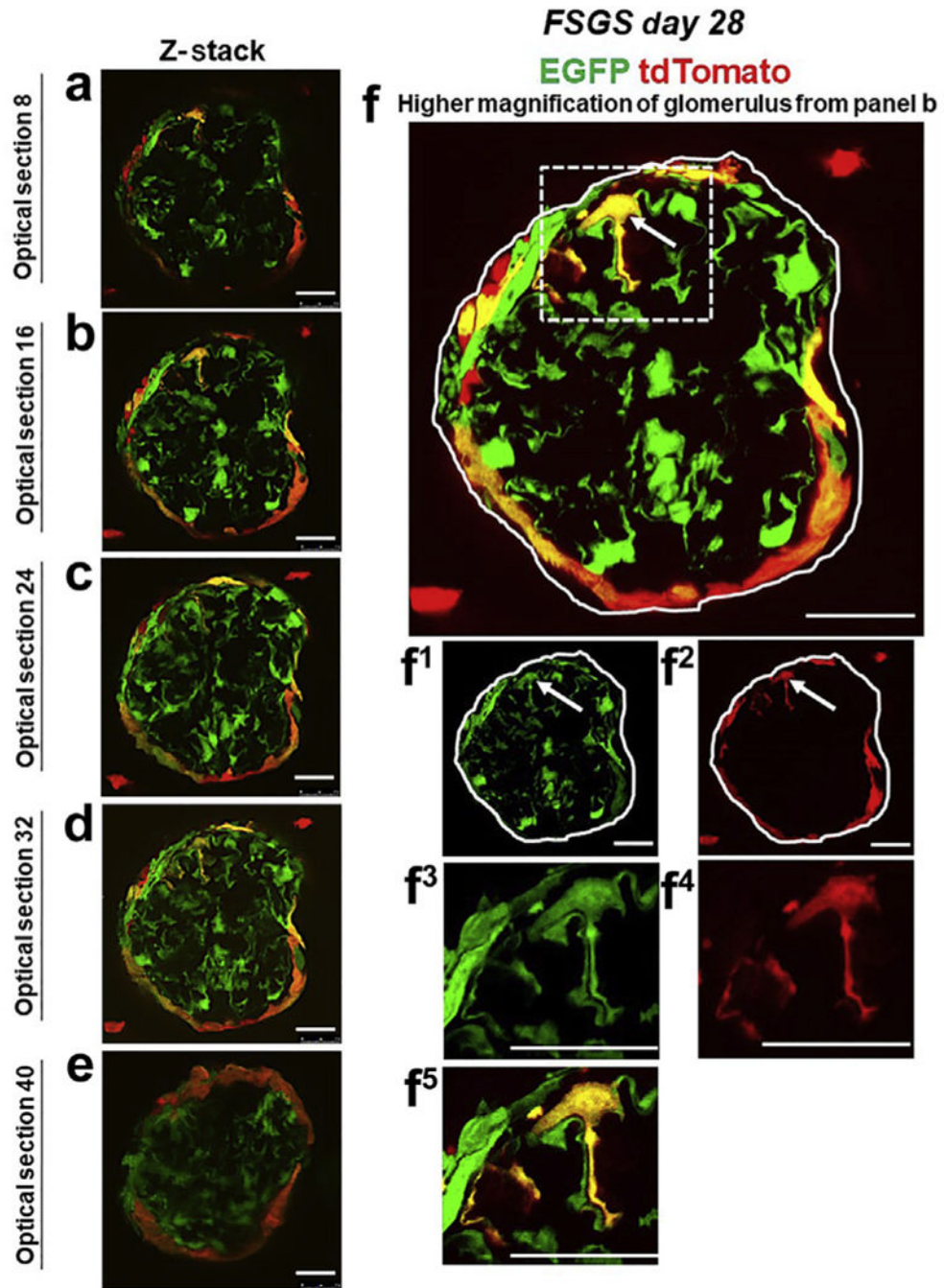


**Figure 3].** tdTomato<sup>+</sup> parietal epithelial cells (PECs) on the glomerular tuft at focal segmental glomerulosclerosis (FSGS) day 28 show genetic evidence of transdifferentiation toward a podocyte fate.

(a–f) Consecutive confocal optical images compiled as a Z-stack through a glomerulus at FSGS day 28 show enhanced green fluorescent protein (EGFP; green), tdTomato (red), and merge (yellow, solid arrows show example). Yellow cells are detected on the glomerular tuft, and the density of tdTomato<sup>+</sup> PECs along Bowman’s capsule is substantially reduced as cells move from Bowman’s capsule to the glomerular tuft. (f) A higher magnification of optical section 16 from the Z-stack. Single fluorescent channels of the inset marked by the

dashed box show EGFP (**f1**) and tdTomato (**f2**). Further magnified images of the area marked by the dashed box with a migrated tdTomato<sup>+</sup> EGFP<sup>+</sup> PEC are shown in following panels: (**f3**) EGFP, (**f4**) TdTomato, and (**f5**) merge. Antibodies were not required to detect EGFP and tdTomato reporters. These results provide genetic proof that at FSGS day 28, a subset of tdTomato<sup>+</sup> PECs that migrated to the glomerular tuft transdifferentiate to a podocyte fate. Bars = 25  $\mu$ m or 5  $\mu$ m (insets).

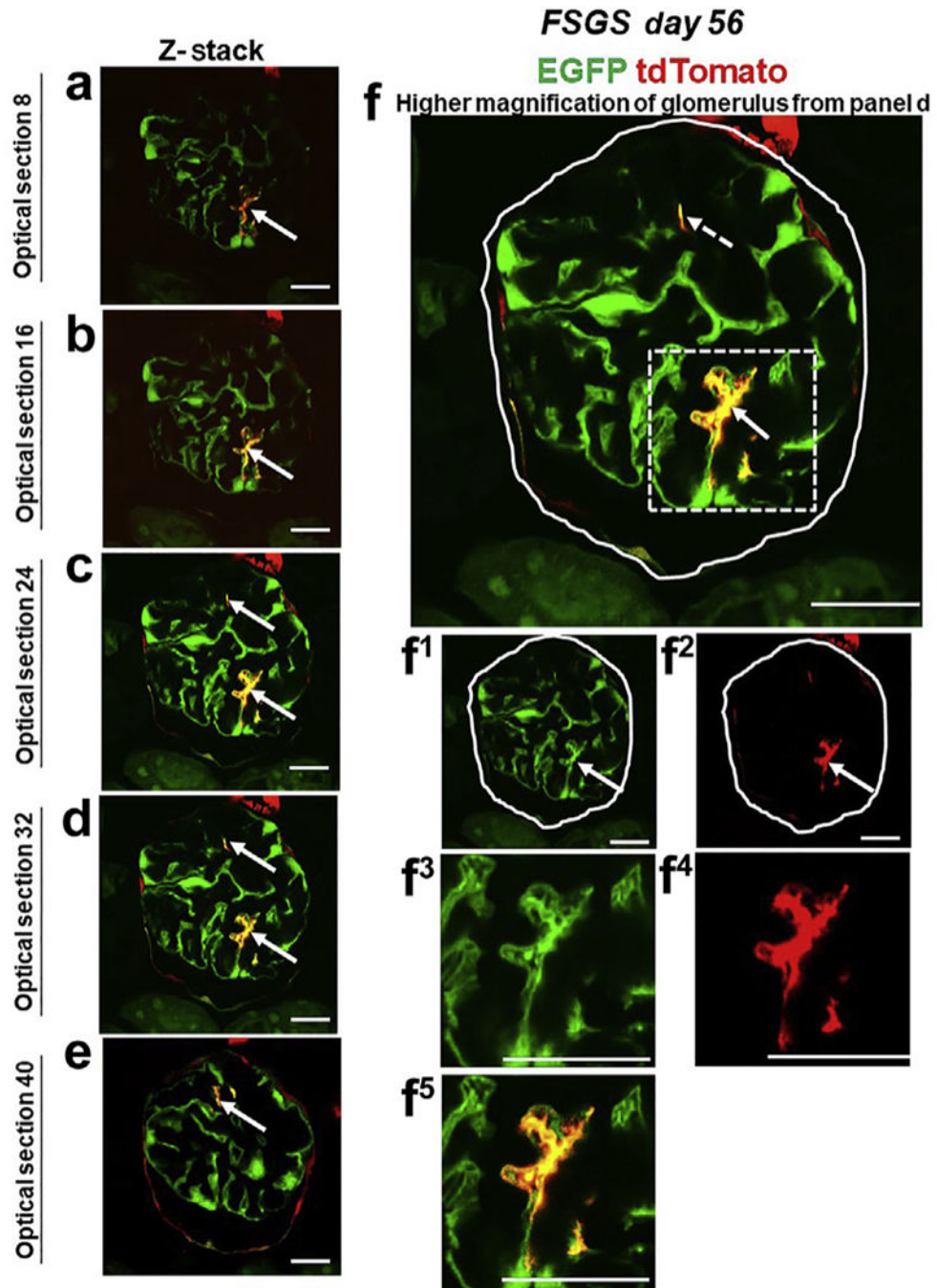


**Figure 4.**  $tdTomato^+$  parietal epithelial cells (PECs) on the glomerular tuft at focal segmental glomerulosclerosis (FSGS) day 56 show genetic evidence of transdifferentiation toward a podocyte fate.

(a-e) Consecutive confocal optical images from top to bottom through a glomerulus compiled as a Z-stack of *PEC-rtTA* / *LC1* / *tdTomato* / *Nphs1-FLPo* / *FRT-EGFP* (PEC-PODO) mice given doxycycline at FSGS day 56 show enhanced green fluorescent protein (EGFP; green), tdTomato (red), and merge (yellow). Yellow cells are detected on the glomerular tuft and are particularly visible in panels b-d. Panels c-e show evidence of another yellow cell. (f) A higher magnification of optical section 32 from the Z-stack. Single

fluorescent channels of the inset marked by the dashed box show EGFP (**f1**) and tdTomato (**f2**). Further magnified images of the area marked by the dashed box with a migrated tdTomato<sup>+</sup> EGFP<sup>+</sup> PEC are shown in panels (**f3**) EGFP, (**f4**) TdTomato, and (**f5**) merge. Antibodies were not required to detect EGFP and tdTomato reporters. These results provide genetic proof that at FSGS day 56, a subset of tdTomato<sup>+</sup> PECs that migrated to the glomerular tuft transdifferentiate to a podocyte fate. Bars = 25 μm or 5 μm (insets).

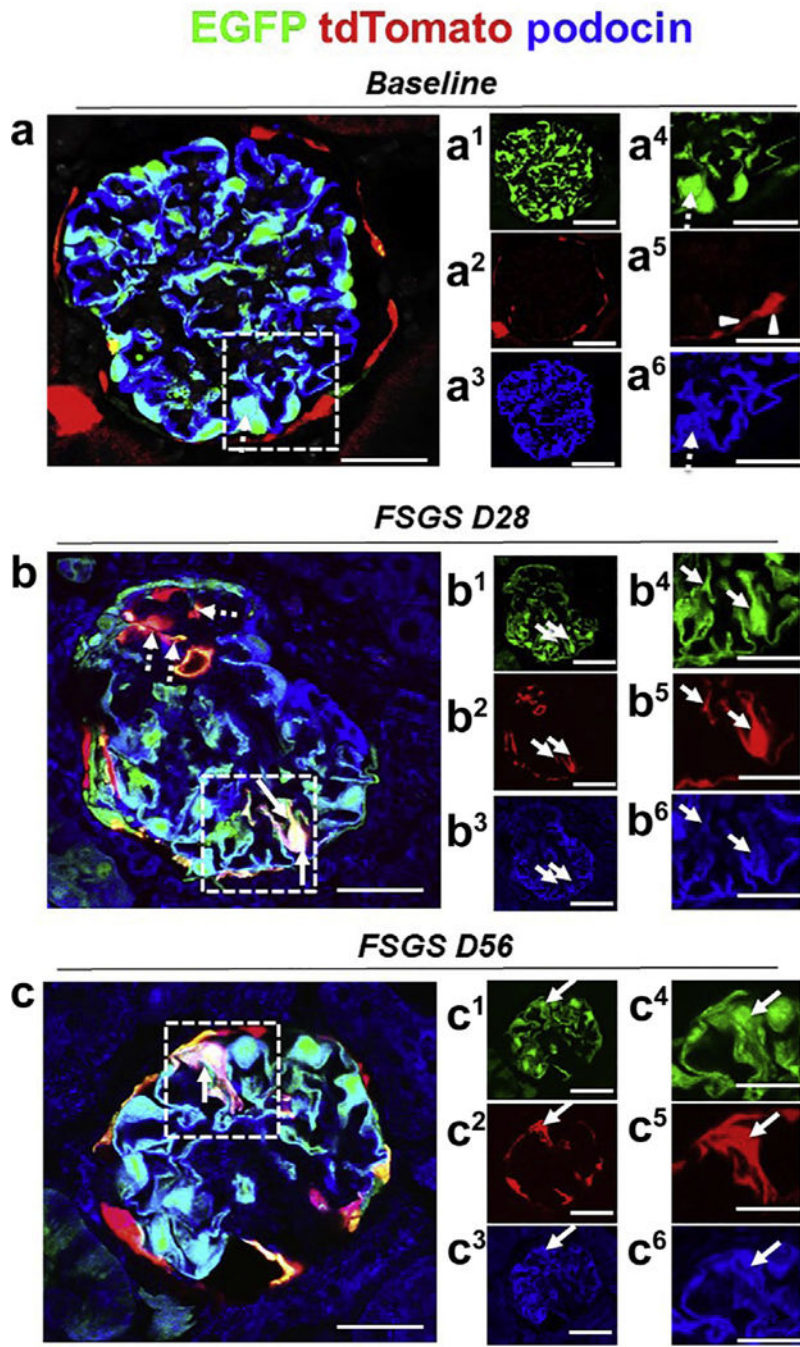


**Figure 5]. A subset of tdTomato<sup>+</sup> parietal epithelial cells (PECs) that have migrated to the tuft after podocyte loss acquire a podocyte fate and begin to express the podocyte protein podocin. Representative confocal micrographic images of enhanced green fluorescent protein (EGFP)<sup>+</sup> (green), tdTomato (red), and podocin (blue) at baseline, day 28 (D28), and day 56 (D56) of focal segmental glomerulosclerosis (FSGS). Panels labeled with numbers 1 and 4 represent EGFP (green); 2 and 5, tdTomato (red); and 3 and 6, immunofluorescence co-stained with the podocyte marker podocin (blue). (a) At baseline, the majority of EGFP<sup>+</sup> cells (a1, a4) co-localized with podocin (a3, a6) (marked with dashed arrows), and tdTomato<sup>+</sup> PECs are**

Author Manuscript

Author Manuscript

Author Manuscript

Author Manuscript



detected along Bowman's capsule (**a2, a5**) (marked with white arrowheads). (**b**) At day 28 of FSGS, a tdTomato<sup>+</sup> PEC (**b2, b5**) (marked with solid arrows in dashed box) has migrated onto the glomerular tuft, has transdifferentiated to a podocyte fate, and co-expresses EGFP (green) (**b1, b4**) and podocin (blue) (**b3, b6**), creating a pink/yellow color (**b**). (**c**) At FSGS day 56, a tdTomato<sup>+</sup> PEC (**c2, c5**) has migrated onto the glomerular tuft, has transdifferentiated to a podocyte fate, and co-expresses EGFP (green) (**c1, c4**) and podocin (blue) (**c3, c6**), creating a pink/yellow color (**c**, marked with solid arrows). Bars = 25  $\mu$ m or 5  $\mu$ m (insets).

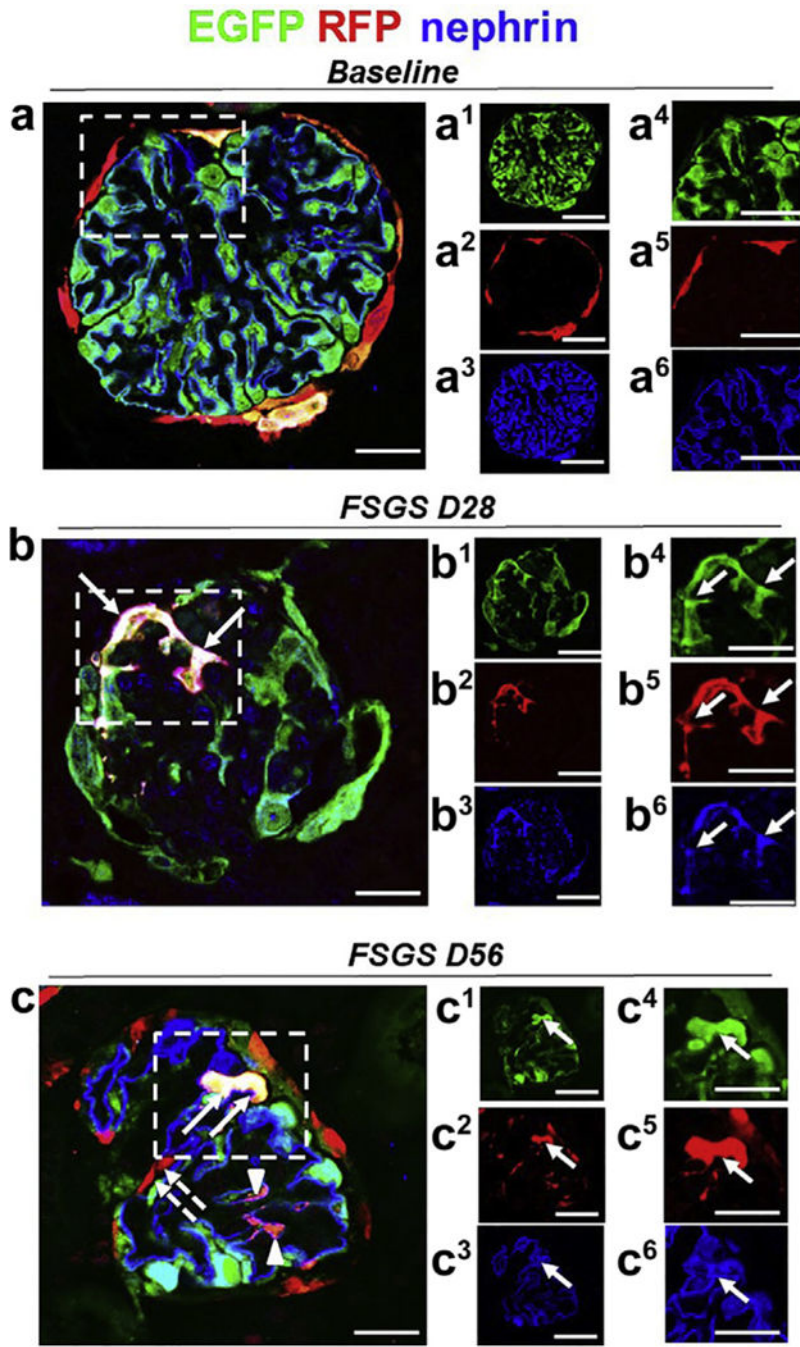


**Figure 6.** A subset of tdTomato<sup>+</sup> parietal epithelial cells (PECs) that have migrated to the tuft after podocyte loss acquire a podocyte fate and begin to express the podocyte protein nephrin. Representative confocal images of immunostaining at baseline, day 28 (D28), and day 56 (D56) of focal segmental glomerulosclerosis (FSGS). Panels labeled with numbers 1 and 4 represent enhanced green fluorescent protein (EGFP; green, podocytes); 2 and 5, tdTomato (red); and 3 and 6, nephrin (blue). (a) At baseline, the majority of EGFP<sup>+</sup> cells (a1, a4) colocalized with nephrin (a3, a6), and tdTomato<sup>+</sup> PECs are detected along Bowman’s capsule (a2, a5). (b) At day 28 of FSGS, a tdTomato<sup>+</sup> PEC (b2, b5) (marked with solid arrows in the

dashed box) has migrated onto the glomerular tuft, transdifferentiated to a podocyte fate, and co-expresses EGFP (green) (**b1, b4**) and nephrin (blue) (**b3, b6**), creating a pink/white color (**b**). (**c**) At FSGS day 56, a subpopulation of tdTomato<sup>+</sup> PECs have migrated to the glomerular tuft and remained red (marked with dashed arrows). A tdTomato<sup>+</sup> PEC (**c2, c5**) has migrated onto the glomerular tuft, transdifferentiated to a podocyte fate, and co-expresses EGFP (green) (**c1, c4**) and nephrin (blue) (**c3, c6**), creating a pink/white color (**c**, marked with solid arrows). Bars = 25  $\mu$ m or 5  $\mu$ m (insets).

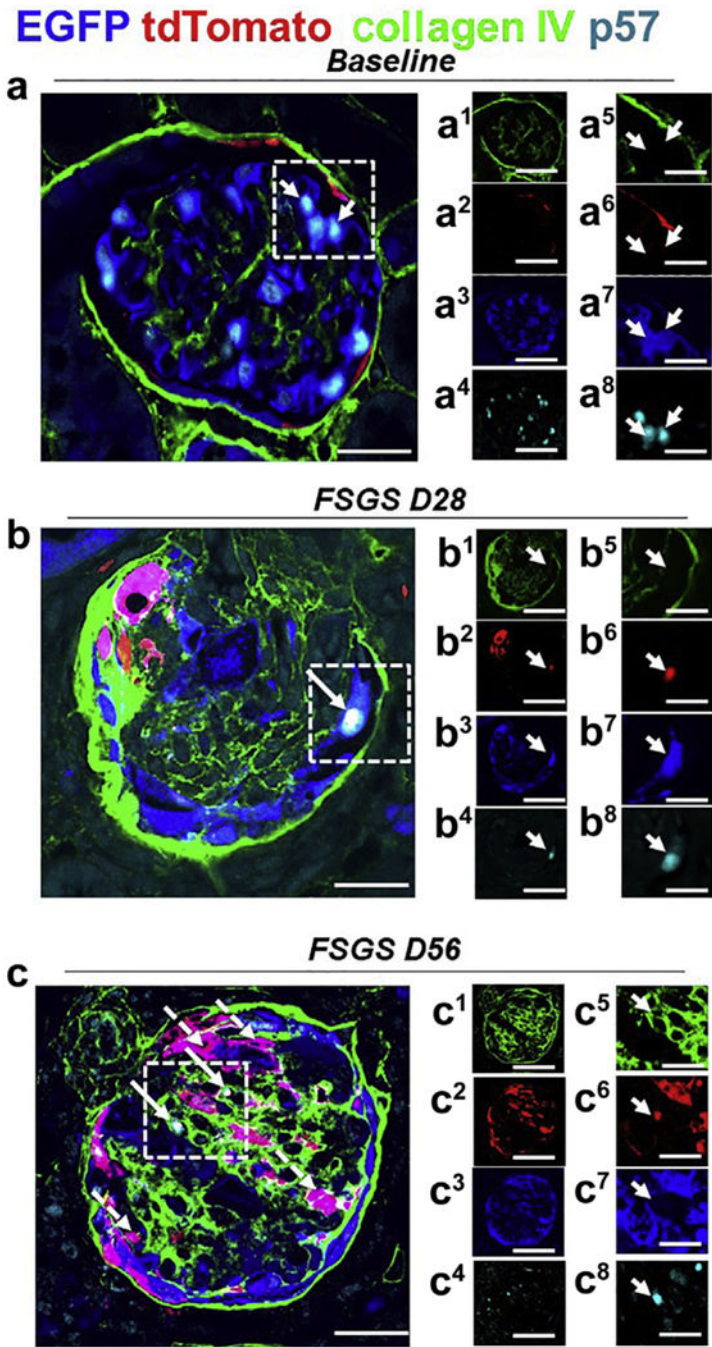


**Figure 7]. A subset of tdTomato<sup>+</sup> parietal epithelial cells (PECs) that have migrated to the tuft after podocyte loss acquire a podocyte fate and begin to express the podocyte protein p57. Representative images of 4-color immunostaining at baseline, day 28 (D28), and day 56 (D56) of focal segmental glomerulosclerosis (FSGS). The panels in the 2 right columns show individual colors for collagen IV (green), tdTomato (red), enhanced green fluorescent protein (EGFP; blue), and p57 (cyan); the column on the far right shows higher magnification images of the area highlighted with the dashed boxes. (a) At baseline, the majority of EGFP<sup>+</sup> cells (blue) (a3, a7) co-localized with p57 (a4, a8) and tdTomato<sup>+</sup> PECs**

(red) (a2, a6) are detected along Bowman’s capsule, delineated by collagen IV (green) (**a1, a5**). (**b**) At day 28 FSGS, a tdTomato<sup>+</sup> PEC (red) (**b2, b6**) has migrated to the glomerular tuft, transdifferentiated to a podocyte fate, and co-expresses EGFP (blue) (**b3, b7**) and p57 (cyan) (**b4, b8**), creating a white color (**b**), marked with a solid arrow. Bowman’s capsule and glomerular tuft are delineated with collagen IV (green) (**b1, b5**). (**c**) At day 56 FSGS, a number of tdTomato<sup>+</sup> PECs (red) (**c2, c6**) have migrated to the glomerular tuft, transdifferentiated to a podocyte fate, and co-expressed EGFP (blue) (**c3, c7**; **c**, magenta color, dashed arrows). A subpopulation of those cells co-stained for the podocyte marker p57 (cyan) (**c4, c8**) (**c**, white color, solid arrows). Bowman’s capsule and the glomerular tuft are delineated with collagen IV (green) (**c1, c5**). Bars = 25  $\mu$ m or 5  $\mu$ m (insets).

Author Manuscript

Author Manuscript

Author Manuscript

Author Manuscript

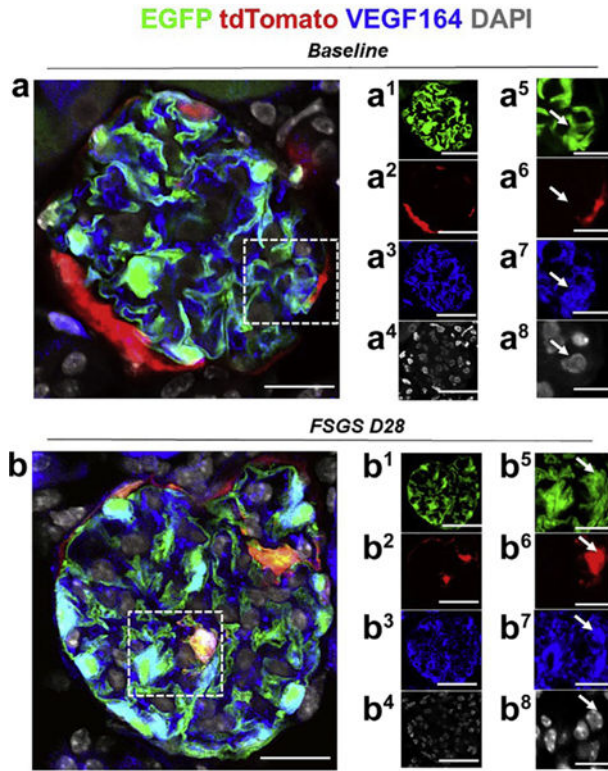


**Figure 8]. Migrated tdTomato<sup>+</sup> parietal epithelial cells (PECs) *de novo* express podocyte-specific VEGF164 in experimental focal segmental glomerulosclerosis (FSGS).**  
 Representative images of 4-color immunostaining at baseline and day 28 (D28) FSGS. The panels in the right 2 columns show individual colors for enhanced green fluorescent protein (EGFP; green, podocyte reporter), tdTomato (red, PEC reporter), VEGF164 (blue, podocyte-specific vascular endothelial growth factor [VEGF] variant) and 4,6-diamidino-2-phenylindole (DAPI; white/gray) to mark nuclei; the panels on the far right show higher magnification images of the area highlighted with the dashed boxes. **(a)** At baseline, the majority of EGFP<sup>+</sup> cells (green) **(a1, a5)** co-localized with VEGF 164 (blue) **(a3, a7)**, and tdTomato<sup>+</sup> PECs (red) are detected along Bowman’s capsule **(a2, a6)**, nuclei as marked by DAPI (white) **(a4, a8)**. **(b)** At day 28 FSGS, a tdTomato<sup>+</sup> PEC (red) **(b2, b6)** has migrated to the glomerular tuft, transdifferentiated to a podocyte fate, and co-expresses EGFP (green) **(b1, b5)** and VEGF 164 (blue) **(b3, b7)**, nuclei as marked by DAPI (white) **(b4, b8)**, creating a pink/yellow color **(b)**. Bars = 25 μm or 5 μm (insets).

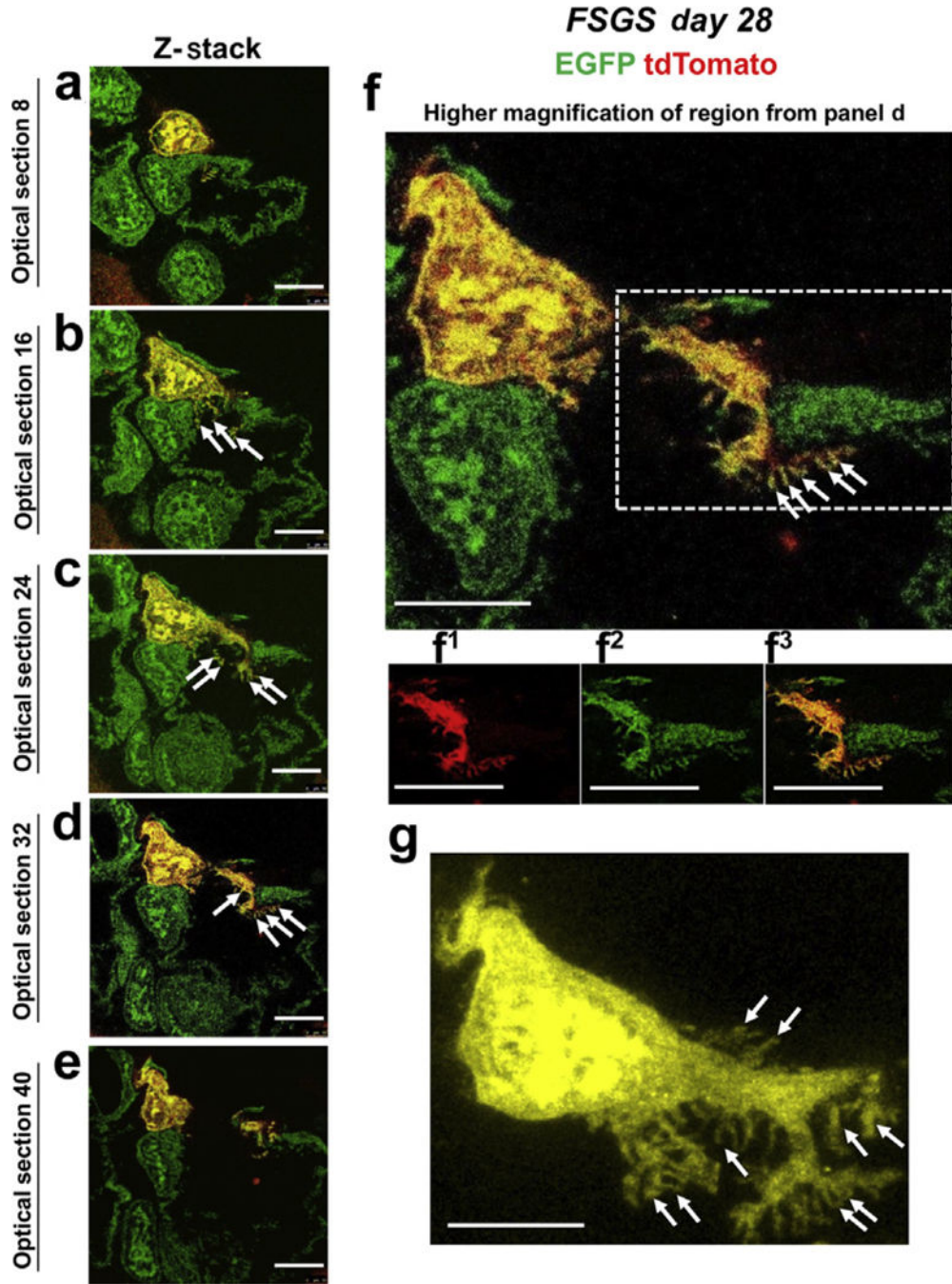


**Figure 9). Ultrastructural features of podocyte derived from parietal epithelial cell (PEC) origin in experimental focal segmental glomerulosclerosis (FSGS).**

(a–e) Z-stack of confocal images of a region of a glomerulus from a *PEC-rtTA/LC1/tTomato*/*Nphs1-FLPo*/*FRT-EGFP* (PEC-PODO) mouse at day 28 FSGS. A tdTomato<sup>+</sup> PEC has migrated to the glomerular tuft, transdifferentiated to a podocyte fate, and co-expresses enhanced green fluorescent protein (EGFP; green), creating a yellow color. (b) There are clear interdigitations (marked with solid white arrows) between the red/yellow PEC and the native green podocytes that have remained on the glomerular basement membrane. (f) A

higher magnification of optical section 32. Primary, secondary, and minor process formation of the newly generated podocyte is highlighted in the dashed box; panels with numbers show tdTomato (**f1**, red), EGFP (**f2**, green), and merge (**f3**, yellow). (**g**) Higher-magnification image of a podocyte derived from PEC lineage (yellow). Note that main processes are formed from the lateral branches (marked with solid arrows). Bars = 25  $\mu\text{m}$  or 5  $\mu\text{m}$  (inset) and are in pre-expansion dimensions.

Author Manuscript

Author Manuscript

Author Manuscript

Author Manuscript



### Empirical Modeling of Podocyte Injury Dynamics: *SIR Model*

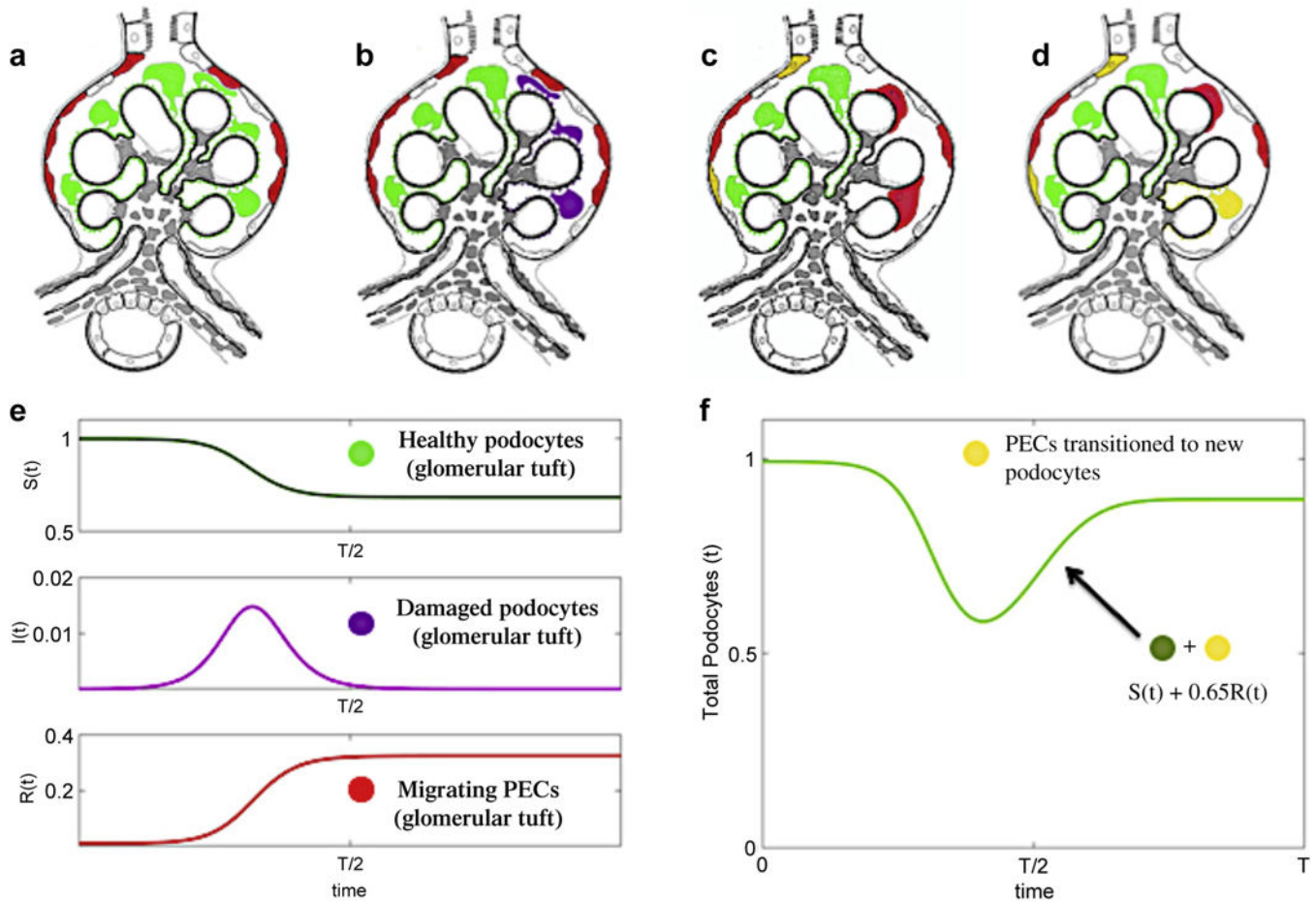


**Figure 10|.** Empirical modeling of podocyte injury dynamics: susceptible, infected, and recovery (SIR) model.

(a-d) Schema of parietal epithelial cell (PEC) migration from Bowman's capsule to the glomerular tuft. (a) Labeling of PECs (red) on Bowman's capsule and podocytes (green) within the normal glomerular tuft before disease onset. (b) After induction of focal segmental glomerulosclerosis (FSGS), podocytes on the glomerular tuft are injured/lost (purple). (c) Podocyte injury/loss induces migration of PECs from Bowman's capsule to the glomerular tuft (red). (d) Approximately 65% of red PECs convert (transdifferentiate) to yellow podocytes. (e) SIR dynamics for  $b = 0.4$  and  $k = 1/3$ . The dynamics mirror qualitatively what is observed for injured podocytes and their recovery through the migration of PECs into the glomerulus and their transdifferentiation to podocytes. Note the color coding of the dynamics is consistent with panels (a-d). (f) Graphical illustration of podocyte number change during FSGS: total number of podocytes in the glomerular tuft, which is a sum of the green and yellow podocytes.